Submitted: 05 February, 2024 Accepted: 08 May, 2024 Published: 30 September, 2024 DOI:10.22514/jomh.2024.154

ORIGINAL RESEARCH

JOMH Journal of Men's Health

The significance of PI-RADS v2.1 score combined with quantitative parameters of DWI and DCE-MRI in differentiating between benign prostatic hyperplasia and prostate cancer

Chengcheng Gao[1], Yangsheng Li[1], Chunfeng Hu[1,2], Gang Tao[3], Jingyi Huang[4,*]

[1]Department of Radiology, Hangzhou First People's Hospital, 310006 Hangzhou, Zhejiang, China
[2]The Fourth School of Clinical Medicine, Zhejiang Chinese Medicine University, 310053 Hangzhou, Zhejiang, China
[3]Department of Oncology, Zhejiang Medical and Health Group Hangzhou Hospital, 310022 Hangzhou, Zhejiang, China
[4]Department of Radiology, Zhejiang Medical and Health Group Hangzhou Hospital, 310022 Hangzhou, Zhejiang, China

***Correspondence**
hjy@zyjhzyy.com
(Jingyi Huang)

Abstract

This study investigates the efficacy of the Prostate Imaging Reporting and Data System version 2.1 (PI-RADS v2.1) score combined with quantitative metrics from Diffusion Weighted Imaging (DWI) and Dynamic Contrast Enhancement Magnetic Resonance Imaging (DCE-MRI) in differentiating between benign prostatic hyperplasia (BPH) and prostate cancer (PCa). The data of 65 patients with prostate diseases were retrospectively analyzed, and they were divided into a BPH group (n = 34) and a PCa group (n = 31). All patients underwent a multiparametric MRI (mpMRI) examination, which included conventional MRI, DWI and DCE-MRI scans. Variables analyzed included the PI-RADS v2.1 score, apparent diffusion coefficient (ADC), volume transfer constant (K^{trans}), rate constant (K_{ep}) and extravascular space volume ratio (V_e). The diagnostic performance of the PI-RADS v2.1 score, DWI, DCE-MRI and their combined metrics in differentiating BPH from PCa was assessed using Receiver Operating Characteristic (ROC) curve analysis. The results demonstrated that the PI-RADS v2.1 scores, K^{trans} and K_{ep} values of the PCa group were significantly higher than those of the BPH group ($p < 0.001$), while the ADC value of the PCa group was significantly lower than the BPH group ($p < 0.001$). No significant difference was observed in the V_e value between the two groups ($p = 0.596$). ROC analysis indicated that the area under the curve (AUC) values for the PI-RADS v2.1 score, ADC, K^{trans}, K_{ep}, V_e and their combination parameters were 0.824, 0.916, 0.903, 0.904, 0.625 and 0.990, respectively, with the combined parameters showing higher sensitivity and specificity than any single parameter. These findings suggest that the PI-RADS v2.1 score, along with DWI and DCE-MRI sequences, are valuable tools for differentiating BPH from PCa. The quantitative parameters, including ADC, K^{trans} and K_{ep} values, offer significant imaging references for clinical assessment, and the combination parameters can significantly enhance diagnostic accuracy.

Keywords

Magnetic resonance imaging; Diffusion weighted imaging; Dynamic contrast enhancement; Benign prostatic hyperplasia; Prostate cancer

1. Background

Benign prostatic hyperplasia (BPH) and prostate cancer (PCa) are common diseases affecting the male population [1]. Recent trends have shown an increase in the incidence of prostate tumors, particularly attributed to the aging population in China. The incidence of these conditions in elderly men is notably high, ranking first in developed countries and sixth in China, posing a significant threat to men's health [1, 2]. Therefore, it is important to accurately differentiate between BPH and PCa, as prompt diagnosis and timely treatment of PCa significantly influence patient prognosis [3].

Magnetic Resonance Imaging (MRI) is a non-invasive imaging modality offering high-resolution visuals of soft tissues. It enables multi-angle, multi-sequence, and multiparametric examination of lesions. It is commonly used in the screening, localization and staging of PCa [4]. The Prostate Imaging Reporting and Data System (PI-RADS) serves as a vital protocol for MRI-based assessment and diagnosis of prostate ailments [5]. Its most recent update, PI-RADS version 2.1 (v2.1), introduced in 2019, revised the specifications for multiparametric MRI (mpMRI) examinations of the prostate [6] and emphasizes the analysis of multiple sequence parameters, including Diffusion Weighted Imaging (DWI), Dynamic Con-

trast Enhanced (DCE)-MRI, and conventional T2-Weighted Imaging (T2WI) sequence.

DWI provides insights into the diffusion properties of living tissues, with the apparent diffusion coefficient (ADC) serving as a quantitative indicator of the diffusion restriction of water molecules within the intercellular space [7]. In PCa, the accelerated growth and dense packing of malignant cells lead to diminished extracellular space, constraining the dispersion of water molecules. Consequently, this presents as elevated signal intensity on DWI sequences and reduced signal intensity on ADC maps. Conversely, BPH does not significantly increase the cell density per unit volume, allowing for more unrestricted diffusion of water molecules.

DCE-MRI is an MRI technique that reduces the T1 signal in the scanned area after intravenous injection of the contrast medium and continuously collects multi-temporal information [8]. DCE-MRI primarily assesses microcirculation perfusion and blood vessel wall permeability. PCa is characterized by increased blood flow and neoangiogenesis, which facilitates the rapid entry and exit of the contrast medium into and out of the tissues and vascular lumen, thereby serving as a critical discriminator between PCa and BPH [9]. The quantitative parameters for DCE-MRI include the volume transfer constant (K^{trans}), rate constant (K_{ep}) and extravascular space volume ratio (V_e), which reflect the intrinsic pathological and microvascular characteristics of tissues [8].

In this study, we structured our approach around the PI-RADS v2.1 score and quantitative parameters derived from DWI and DCE-MRI. Our objective was to differentiate between BPH and PCa and assess the clinical relevance of combining these parameters for improving the diagnostic efficacy for PCa.

2. Materials and methods

2.1 Patient population

During this investigation, we continuously gathered clinical and medical imaging data from 65 patients diagnosed with prostate diseases who were admitted to our hospital between January 2020 and December 2022. The inclusion criteria were: (1) Diagnosis confirmed by surgical excision or trans-perineal ultrasound-guided prostate biopsy after MRI; (2) Availability of complete clinical data and pathological examination results; and (3) Had prostate MRI scan sequences, including T2WI, DWI and DCE-MRI. The exclusion criteria were: (1) Patients with a history of prostate puncture, surgery, radiotherapy, or endocrine therapy before MRI examination; and (2) Poor quality MRI images that affected diagnosis and scoring. Ultimately, a total of 65 patients, comprising 34 BPH patients (BPH group) and 31 PCa patients (PCa group), were identified as eligible for study analysis.

2.2 MRI acquisition protocol

Prostate MRI examinations were conducted utilizing a 3T whole-body MRI scanner fitted with an eight-channel phased-array coil (Verio, Siemens Healthcare, Erlangen, Germany). Before the examination, patients were required to rest for 6 hours and ensure a sufficiently full bladder. During the scan, patients were positioned supine with feet first. The MRI protocol included axial, coronal and sagittal T2WI, DWI and DCE-MRI. A contrast agent, gadolinium diamine (Omniscan, General Electric Pharmaceutical (Shanghai) Co., Ltd., Shanghai, China; approval number Guoyao Zhunzi J20140164, dosage form: 20 mL: 5.74 g), was administered intravenously through the elbow at a concentration of 0.1 mmol/kg and a flow rate of 3 mL/s. The details of prostate MRI acquisition scan parameters are summarized in Table 1.

2.3 Image analysis

Two independent radiologists with 6 and 8 years of experience in prostate diagnosis reviewed all MRI images in a double-blind manner using PI-RADS v2.1 to score the images of index lesions in each sequence. For patients with multiple lesions, only the lesion assigned the highest PI-RADS score was included for statistical analysis. In instances of scoring discrepancies, the radiologists engaged in discussions to deliberate on the results until a consensus regarding the final score was achieved.

The DCE-MRI images were processed using the Omni-Kinetics software (Version 2.0.10, GE Healthcare, Chicago, IL, USA). The pharmacokinetic analysis was performed using the two-chamber model (Extended-Tofts model) to uniformly select the right external iliac artery as the input artery. The

TABLE 1. Sequence parameters for prostate MRI.

Parameters	T2WI	DWI	DCE-MRI
Sequence	FRFSE	SRE-EPI	3D-VIBE
TR/TE (ms)	4400/96	6400/60	5.0/1.7
Flip angle	160°	170°	15°
FOV (mm × mm)	180 × 180	180 × 180	240 × 190
Matix size	224 × 320	224 × 320	224 × 192
Slice thickness (mm)	3.0	3.0	3.0
NEX	4	4	4
Other	/	*b*-values = 0, 800 s/mm^2	Temporal resolution <10 s, total scan time of 300 s

T2WI: T2-weighted imaging; DWI: diffusion-weighted imaging; DCE-MRI: dynamic contrast enhancement-magnetic resonance imaging; TR: time of repetition; TE: time of echo; FOV: field of view; NEX: number of excitations.

quantitative parameters of DCE-MRI, including K^{trans}, K_{ep} and V_e, were calculated. Referring to the corresponding T2WI slice locations, the radiologists visually aligned the ADC maps and identified the region of interest (ROI). Three measurements were conducted for each ROI to determine an average value, carefully avoiding areas with blood vessels, fat, calcification, *etc*.

2.4 Statistical analysis

Data analysis was performed using the SPSS statistical software (version 25, SPSS Inc., Armonk, NY, USA). The independent samples *t*-test was utilized to evaluate normally distributed continuous variables. Differences in the PI-RADS v2.1 score of the lesions and quantitative parameters (K^{trans}, K_{ep}, V_e, ADC values) between the benign and malignant groups were compared. Employing the pathological results as the reference standard, the area under the curve (AUC) of the receiver operating curve (ROC) was utilized to quantify the predictive accuracy of each parameter in differentiating between the BPH group and the PCa group. The Youden index, calculated as sensitivity plus specificity minus one, was utilized to determine the optimal diagnostic cut-off value, where the sensitivity and specificity of these parameter values were maximized. A *p*-value of less than 0.001 was deemed statistically significant for all tests.

3. Results

3.1 Patient clinical characteristics

The study encompassed data from a total of 65 patients diagnosed with prostate disease. The BPH group comprised 34 patients, aged between 56 and 88 years, with a mean age of 73.06 ± 8.98 years. In this group, 7 lesions were identified in the peripheral zone, while the remaining lesions were located in the transition zone. The PCa group comprised 31 patients, aged between 65 and 95 years, with a mean age of 77.94 ± 9.13 years. Among these patients, 5 lesions were situated in the transition zone, 1 lesion was detected in the anterior fibromuscular stroma, and the rest of the lesions were either in the peripheral zone or spanned both the peripheral and transition zones. The age disparity between the two groups did not reach statistical significance ($p = 0.034$).

3.2 MRI findings and PI-RADS v2.1 score of BPH and PCa patients

All 34 BPH cases had enlarged prostate size, and 30 of them protruded into the bladder. The T2WI sequence revealed significant enlargement of the central gland area, presenting a heterogeneous signal within the lesion and compression of the peripheral band. DWI sequences identified 2 lesions with slightly higher signal intensity, while the remaining lesions displayed isointense signals. DCE-MRI sequences illustrated varying patterns of uneven and continuous enhancement across the lesions. Comparatively, among the 31 patients with PCa, 7 exhibited well-defined nodular and lenticular lesions with low signal intensity, with 5 of these located in the peripheral zone and 2 in the anterior fibromuscular stroma. The other lesions were irregular in shape with unclear boundaries, and in the T2WI sequence, the signals of some lesions were not significantly reduced. DWI sequences revealed that 21 PCa patients had lesions with slightly high or high signal intensity; ADC values were slightly low or low, whereas the remaining 10 patients presented with isointense signals. In the DCE-MRI sequence, 25 lesions demonstrated rapid and pronounced enhancement in the early phase, with clear demarcation in the middle and late phases. Six cases showed persistent enhancement. Moreover, there were 5 instances of pelvic lymph node metastases and 3 of bone metastases. The difference in PI-RADS v2.1 scores between the BPH and PCa groups was statistically significant (2.240 ± 0.923 *vs.* 3.520 ± 0.890, $p < 0.001$). The MRI images of a BPH case and a PCa case are shown in Fig. 1.

3.3 Comparison of ADC values and quantitative parameters of DCE-MRI between BPH group and PCa group

The ADC value of the PCa group was found to be significantly lower than that of the BPH group ($t = 6.929$, $p < 0.001$). In addition, the K^{trans} and K_{ep} values of the PCa group were higher than those of the BPH group, and the difference was statistically significant ($t = -8.302$, $p < 0.001$, $t = -6.446$, $p < 0.001$, respectively), while there was no significant difference in V_e between the two groups ($t = -0.533$, $p > 0.001$) (Table 2).

3.4 Diagnostic performance analysis of PI-RADS v2.1 score, ADC value, quantitative parameters of DCE-MRI and their combination parameters

The AUC value of PI-RADS v2.1 score was 0.824, and the AUC value of ADC, K^{trans}, K_{ep} and V_e value was 0.916, 0.903, 0.904 and 0.625, respectively. The above parameters were combined for diagnosis, and the AUC value of the combination was found to be 0.990. Then, the ROC curves were plotted, and the cut-off values, sensitivity, specificity, Youden and AUC values of each item are determined in Table 3 and Fig. 2.

4. Discussion

Prostate diseases are more common in middle-aged and elderly men [10]. PCa is one of the most common malignant tumors among males, ranking second in incidence rates for male malignancies. It poses a significant global public health issue, jeopardizing the life and health of men worldwide [1, 11]. Currently, the clinical diagnosis of PCa primarily depends on serum PSA levels, digital rectal examination, ultrasonography, MRI and needle biopsy. Among them, mpMRI plays an important role in the clinical diagnosis and early assessment of PCa [12]. Clinical guidelines recommend determining the PI-RADS score via mpMRI before conducting a prostate biopsy [6]. In our study, the quantitative parameters, including ADC, K^{trans} and K_{ep} value, can provide imaging reference for clinical value, and the combination parameters can further improve the diagnostic efficiency in differentiating BPH and PCa.

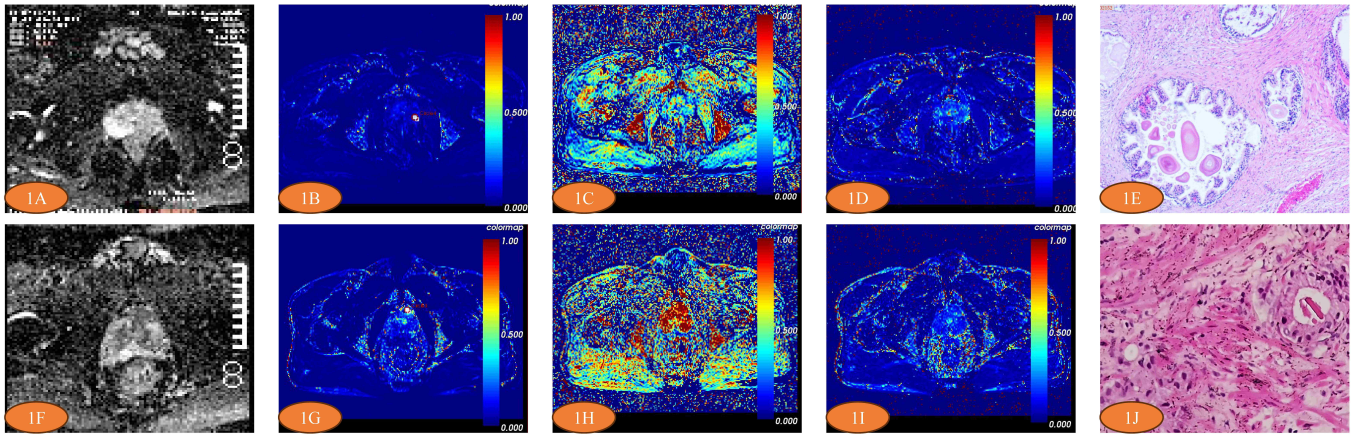

FIGURE 1. A patient with benign prostatic hyperplasia (BPH) and a patient with prostate cancer (PCa). (A–E) Case 1: Male, 65 years old, the lesion is located in the left peripheral band of the prostate. (A) ADC value = 1.329 × 10^{-3} mm^2/s, (B) K^{trans} = 0.072 min^{-1}, (C) K_{ep} = 0.411 min^{-1}, (D) V_e = 0.172, (E) Pathological diagnosis: benign prostatic hyperplasia. (F–J) Case 2: Male, 60 years old, the lesion is located in the preprostatic fibromuscular stromal area. (F) ADC value = 0.630 × 10^{-3} mm^2/s, (G) K^{trans} = 0.283 min^{-1}, (H) K_{ep} = 2.119 min^{-1}, (I) V_e = 0.138, (J) Pathological diagnosis: adenocarcinoma of the prostate, (Gleason score of 4 + 3). ADC: apparent diffusion coefficient; K^{trans}: volume transfer constant; K_{ep}: rate constant; V_e: extravascular space volume ratio.

TABLE 2. The independent samples *t*-test of different items in the BPH group and PCa group.

Items	BPH group (n = 34)	PCa group (n = 31)	*t* value	*p* value
Age/yr	73.059 ± 8.984	77.935 ± 9.132	−2.169	0.034
PI-RADS v2.1 score	2.240 ± 0.923	3.520 ± 0.890	−5.685	<0.001
ADC/×10^{-3} mm^2/s	1.219 ± 0.189	0.868 ± 0.219	6.929	<0.001
K^{trans}/min^{-1}	0.084 ± 0.028	0.231 ± 0.099	−8.302	<0.001
K_{ep}/min^{-1}	0.699 ± 0.298	1.540 ± 0.694	−6.446	<0.001
V_e	0.162 ± 0.100	0.173 ± 0.061	−0.533	0.596

BPH: benign prostatic hyperplasia; PCa: prostate cancer; PI-RADS v2.1: prostate imaging reporting and data system version 2.1; ADC: apparent diffusion coefficient; K^{trans}: volume transfer constant; K_{ep}: rate constant; V_e: extravascular space volume ratio.

TABLE 3. ROC results of PI-RADS v2.1 score, ADC value, quantitative parameters of DCE-MRI and their combination parameters for predicting PCa.

Items	Cut-off	Sensitivity	Specificity	Youden	AUC
PI-RADS v2.1	3.500	0.516	0.941	0.457	0.824
ADC	1.017	0.903	0.912	0.815	0.916
K^{trans}	0.126	0.871	0.912	0.783	0.903
K_{ep}	0.109	0.774	0.971	0.745	0.904
V_e	0.161	0.677	0.412	0.265	0.625
Combination	0.571	0.935	0.971	0.906	0.990

AUC: area under the curve; PI-RADS v2.1: prostate imaging reporting and data system version 2.1; ADC: apparent diffusion coefficient; K^{trans}: volume transfer constant; K_{ep}: rate constant; V_e: extravascular space volume ratio.

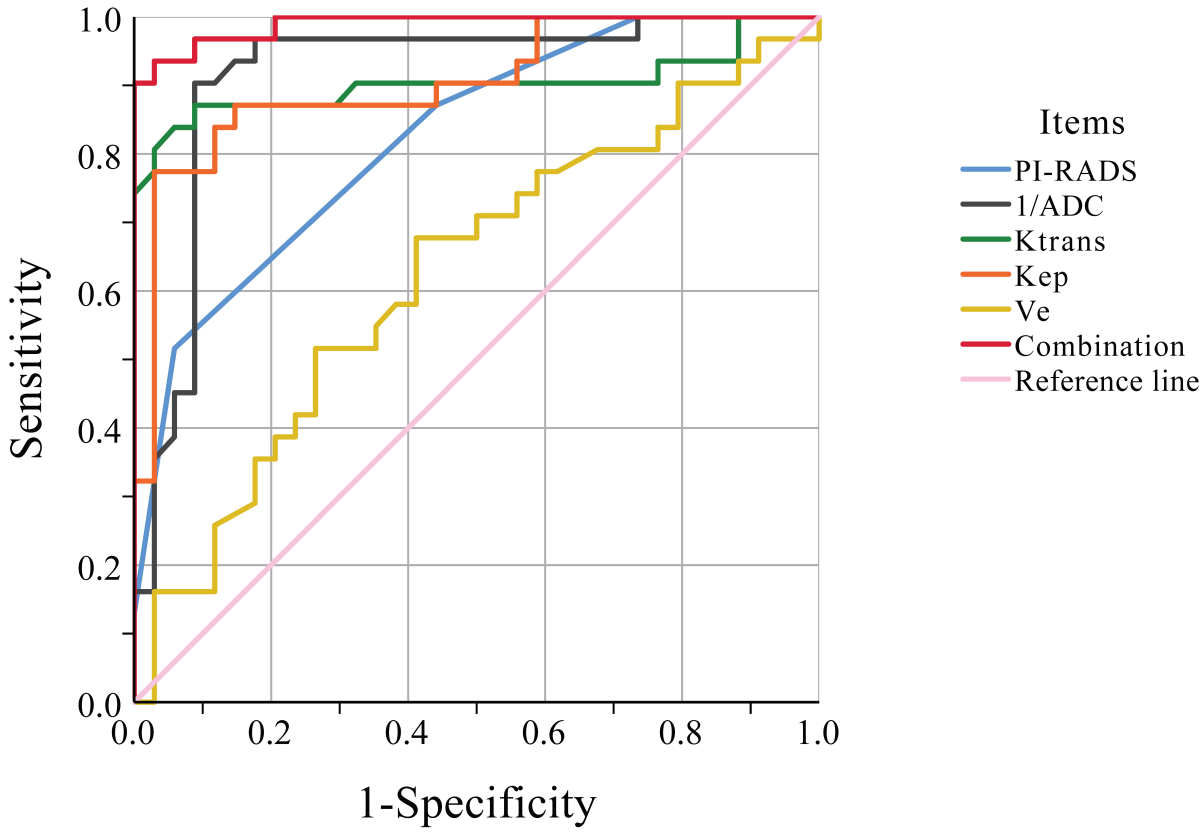

FIGURE 2. ROC curves. The ROC curves for six items' performance to distinguish BPH group and PCa group, respectively. ROC: receiver operating curve; PI-RADS: prostate imaging reporting and data system; ADC: apparent diffusion coefficient; Ktrans: volume transfer constant; Kep: rate constant; Ve: extravascular space volume ratio.

The PI-RADS score was first proposed by the European Society for Genitourinary Radiology (ESUR) in 2012 [5]. Two years later, ESUR and the American College of Radiology (ACR) revised it and launched the second version of the PI-RADS v2 [13]. The latest version of PI-RADS v2.1 has gained rapid and widespread international recognition in the radiology and urology community, and it has been widely used in clinical practice since 2019 [4]. PI-RADS v2.1 primarily focuses on the anatomical structure of the prostate, utilizing T2WI, DWI and DCE-MRI sequences, and further refines the imaging parameters and scoring criteria on the basis of the previous version. In our study, the PI-RADS v2.1 score in the PCa group exhibited a significant elevation compared to the BPH group ($p < 0.001$). The ROC curve analysis for PI-RADS v2.1 yielded an AUC value of 0.824, indicating high diagnostic efficacy, with a sensitivity of 0.516 and a specificity of 0.941. Li M *et al.* [14] reported similar findings in their study of 112 PCa patients and 91 BPH patients, where the AUC of PI-RADS v2.1 was 0.905 (95% confidence interval, 0.844–0.948), sensitivity was 0.962, and specificity was 0.635. The results of our study are somewhat lower than those reported by Li M *et al.* [14], which could be attributed to factors such as a smaller sample size and the type of MRI coil used. Our study involved a patient cohort that was only one-third the size of that in the aforementioned study, leading us to hypothesize that the AUC, sensitivity and specificity could be enhanced with the analysis of a larger sample size in future research. In this investigation, prostate scanning was conducted using a body-phased coil. Although this method was better tolerated by participants, it resulted in a lower signal-to-noise ratio in comparison to scans performed with an intrarectal coil. Traditional T2WI sequences can effectively depict the anatomical structure of the prostate. While PCa typically appears hypointense on T2WI sequences, the lack of contrast with surrounding tissues diminishes its diagnostic utility. Furthermore, other prostate conditions such as inflammation, hemorrhage and calcification can similarly manifest as hypointense, complicating the differentiation based solely on T2WI sequences [15]. In our study, there were 5 cases of BPH located in the peripheral zone, where the T2WI sequence displayed indistinct nodules and patches with slightly low signal intensity, leading to misdiagnoses in imaging interpretation. Moreover, the accuracy of conventional MRI sequence diagnoses is heavily reliant on the radiologist's experience and expertise, introducing the potential for subjective bias [16]. Therefore, there is a pressing need for objective and precise imaging techniques and biomarkers to improve the diagnostic accuracy of PCa.

DWI plays a crucial role in the evaluation assessment of PI-RADS v2.1, providing a non-invasive means to evaluate the diffusion movement of water molecules within tissues [4]. The intensity of the signal in DWI is influenced by various factors, including cell density, integrity of cell membranes, viscosity between cells and the distribution of blood vessels, which are quantitatively represented by the ADC value [17]. ADC serves

as a quantitative indicator of the degree to which the diffusion of water molecules is restricted within tissue. A higher ADC value indicates less restricted diffusion of water molecules, signifying more freedom of movement within the tissue. Conversely, a lower ADC value suggests a greater restriction in water molecule diffusion, often seen in densely cellular or pathological tissues. In PCa, cells proliferate rapidly, leading to increased cellular density, high intercellular viscosity, and reduced extracellular space. Additionally, tumor growth disrupts the normal, water-rich glandular architecture, further restricting water molecule diffusion and resulting in a lower ADC value. On the other hand, in BPH, there is cellular hyperplasia and the glandular structure is densely organized; however, the cellular density and function resemble those of normal prostate tissue, resulting in water molecule diffusion that is more restricted than in normal tissue but less so than in PCa [18]. In our study, the ADC value for the PCa group was significantly lower than that for the BPH group (0.868 $\pm$ 0.219 *vs.* 1.219 $\pm$ 0.189, t = 6.929, $p < 0.001$), and the ADC value was 0.916, with a sensitivity and specificity of higher than 90%, indicating that the ADC value has high diagnostic efficacy in the differentiation of the two diseases. The discrepancy in the ADC cut-off values observed in this study compared to those reported by other researchers may be attributed to variations in the *b* values used in the DWI scanning sequences.

In the current study, the selected *b*-values for DWI were 0 and 800 s/mm^2. Research by some investigators [19] has demonstrated that utilizing *b*-values of 3000 s/mm^2 in DWI on 3T MRI equipment enhanced the suppression of background signal more effectively than *b*-values of 2000 s/mm^2. However, this adjustment does not necessarily lead to improved diagnostic performance in identifying PCa. Moreover, the application of a simplified biparametric MRI protocol, which includes axial T2WI and DWI with b = 2000 s/mm^2, has been shown to achieve diagnostic accuracy comparable to mpMRI in detecting PCa, underscoring the significance of DWI sequences with higher *b*-values [20]. In a study conducted by Tsuruta C *et al.* [21], the use of a range of *b*-values (0, 100, 1000 and 1500 s/mm^2) in DWI was found to be significantly correlated with the classification of PCa, highlighting the important role of DWI parameters in the accurate diagnosis and assessment of PCa.

PCa is characterized by an abundant blood supply, which facilitates the use of DCE-MRI sequences to view microangiogenesis and hemodynamics in tumor tissues [22]. The process of tumor progression in PCa involves a significant increase in vascular density—up to twice or more compared to adjacent normal cells—and enhanced vascular permeability at the lesion sites, which allows for the rapid extravasation of contrast agents [23]. In contrast, BPH does not exhibit the same level of permeability as PCa, resulting in a predominantly slow and continuous pattern of tissue enhancement on DCE-MRI [24]. Distinguishing between these two conditions based solely on the enhancement patterns observed in DCE-MRI can be challenging when relying only on visual analysis by the observer. To facilitate a more quantitative diagnostic approach for prostate diseases using DCE-MRI, the calculation of pharmacokinetic parameters is essential. These parameters quantitatively describe the dynamics of the contrast agent's interaction with the extravascular extracellular space (EES) and its exchange between the vascular and interstitial spaces. The volume transfer constant, K^{trans}, denotes the rate at which the contrast medium transfers from the plasma through the capillaries into the interstitial space per unit time [25]. The rate constant, K_{ep}, signifies the rate at which the contrast medium returns from the interstitial space back into the plasma per unit time. V_e is defined as the volume fraction of the EES outside the blood vessels, with the relationship between these parameters being described by the equation $V_e = K^{trans}/K_{ep}$ [25]. This study showed that the results of K^{trans} and K_{ep} in PCa group were notably higher compared to those in the BPH group, and this disparity was statistically significant (t = −8.302, $p < 0.001$, t = −6.446, $p < 0.001$, respectively). This result can be attributed to the enhanced microvascular permeability and larger endothelial gaps in malignant tissues. This increased permeability facilitates a greater influx and efflux of contrast agents in PCa tissues, a phenomenon not observed to the same extent in BPH due to its similar vascular structure to normal prostate tissue. The ROC curve analysis further supports the diagnostic value of these parameters, with both showing high specificity (specificity of these two parameters was >0.9) and substantial sensitivity (0.871 and 0.774, respectively), indicating their effectiveness in PCa diagnosis, which was close to the results of other researchers [26, 27]. There was no statistically significant difference in the V_e in the PCA and BPH groups (t = −0.533, $p >$ 0.001). Comparatively, the use of V_e values for the diagnosis of PCa is controversial in the literature. Several researchers [28] have reported a lack of statistically significant difference in V_e values between PCa and non-PCa tissues, while other investigations [29] reported that V_e values were higher in PCa than in non-PCa tissues. These discrepancies may be attributed to variations in MRI equipment, sequence parameters, or modeling techniques employed in the respective studies. Currently, there is no consensus among experts nor a definitive cut-off value for these parameters. However, advancements in MRI technology, improved scanning protocols and the expansion of research involving larger sample sizes are expected to enhance the diagnostic abilities of DCE-MRI for PCa in the future.

Each MRI sequence offers unique benefits and limitations, enabling mpMRI to provide comprehensive details on anatomy, tissue structure and blood supply, thereby enhancing diagnostic accuracy. In this research, a combination parameter integrating the PI-RADS v2.1 score, ADC value and quantitative DCE-MRI parameters was evaluated for its efficacy in predicting PCa. The comparison between the diagnostic performance of this composite parameter and that of individual parameters revealed that the AUC for the combination parameter was 0.990, surpassing the diagnostic efficiency of each single parameter with a sensitivity of 0.935 and a specificity of 0.971. These findings align with those of previous studies [30] that used radiomics based on mpMRI, suggesting such an approach can significantly enhance the diagnostic accuracy of PI-RADS v2.1 for PCa.

There are several limitations in our study. Firstly, it is a retrospective analysis conducted at a single institution. Secondly, we investigated the correlation between PI-RADS scores and

the differentiation between benign and malignant conditions, we did not assess the potential diagnostic enhancement from incorporating clinical risk factors with mpMRI for disease differentiation. Lastly, some pathologic results were confirmed by needle biopsy, but due to its high false-negative rate, the diagnostic value of mpMRI might have been underestimated. Thus, prospective studies with larger samples are still needed to validate these results, investigate the addition of clinical risk factors to mpMRI data and optimize MRI sequences for increased diagnostic accuracy [31, 32]. We aim to validate this study's findings and further investigate the diagnostic utility of other quantitative and semi-quantitative DCE-MRI parameters in differentiating between BPH and PCa.

5. Conclusions

In conclusion, the application of PI-RADS v2.1 scoring with quantitative measures from DWI and DCE-MRI holds significant promise for distinguishing PCa from BPH. Moreover, integrating these elements into a combination parameter can increase the utility of the PI-RADS framework, furnishing radiologists with a set of quantitative and standardized metrics, thus enhancing the reliability and accuracy of PCa detection.

AVAILABILITY OF DATA AND MATERIALS

The data presented in this study are available on reasonable request from the corresponding author.

AUTHOR CONTRIBUTIONS

CCG and YSL—designed the research study. YSL and GT—performed the research. CCG, YSL and CFH—analyzed the data. CCG and JYH—wrote the manuscript. All authors read and approved the final manuscript.

ETHICS APPROVAL AND CONSENT TO PARTICIPATE

This study involving human participants was reviewed and approved by the Medical Research Ethics Committee of the Hangzhou First People's Hospital, Hangzhou, Zhejiang Province, China (No. 20231020100000047126O). Written informed consent was provided by the participants' legal guardians or next of kin.

ACKNOWLEDGMENT

We express our gratitude to all the patients for their cooperation and willingness to participate in this study.

FUNDING

This research received no external funding.

CONFLICT OF INTEREST

The authors declare no conflict of interest.

REFERENCES

[1] Siegel RL, Giaquinto AN, Jemal A. Cancer statistics, 2024. CA: A Cancer Journal for Clinicians. 2024; 74: 12–49.

[2] Xia C, Dong X, Li H, Cao M, Sun D, He S, *et al*. Cancer statistics in China and United States, 2022: profiles, trends, and determinants. Chinese Medical Journal. 2022; 135: 584–590.

[3] Chiong E, Saad M, Hamid ARAH, Ong-Cornel AB, Lojanapiwat B, Pripatnanont C, *et al*. Prostate cancer management in Southeast Asian countries: a survey of clinical practice patterns. Therapeutic Advances in Medical Oncology. 2024; 16: 17588359231216582.

[4] Padhani AR, Barentsz J, Villeirs G, Rosenkrantz AB, Margolis DJ, Turkbey B, *et al*. PI-RADS steering committee: the PI-RADS multiparametric MRI and MRI-directed biopsy pathway. Radiology. 2019; 292: 464–474.

[5] Barentsz JO, Richenberg J, Clements R, Choyke P, Verma S, Villeirs G, *et al*. ESUR prostate MR guidelines 2012. European Radiology. 2012; 22: 746–757.

[6] Turkbey B, Rosenkrantz AB, Haider MA, Padhani AR, Villeirs G, Macura KJ, *et al*. Prostate imaging reporting and data system version 2.1: 2019 update of prostate imaging reporting and data system version 2. European Urology. 2019; 76: 340–351.

[7] Arita Y, Yoshida S, Waseda Y, Takahara T, Ishii C, Ueda R, *et al*. Diagnostic value of computed high *b*-value whole-body diffusion-weighted imaging for primary prostate cancer. European Journal of Radiology. 2021; 137: 109581.

[8] Meyer H, Wienke A, Surov A. Can dynamic contrast enhanced MRI predict Gleason score in prostate cancer? A systematic review and meta analysis. Urologic Oncology. 2021; 39: 784.e17–784.e25.

[9] Karaca L, Özdemir ZM, Kahraman A, Çelik H, Kaya S. Assessment of quantitative zonal parameters of prostate gland in discrimination of normal, benign, and malignant conditions: are these the more reliable parameters in the diagnosis of prostate cancer? European Review for Medical and Pharmacological Sciences. 2023; 27: 11122–11130.

[10] Oseni SO, Naar C, Pavlović M, Asghar W, Hartmann JX, Fields GB, *et al*. The molecular basis and clinical consequences of chronic inflammation in prostatic diseases: prostatitis, benign prostatic hyperplasia, and prostate cancer. Cancers. 2023; 15: 3110.

[11] Rebello RJ, Oing C, Knudsen KE, Loeb S, Johnson DC, Reiter RE, *et al*. Prostate cancer. Nature Reviews Disease Primers. 2021; 7: 9.

[12] Rouvière O, Puech P, Renard-Penna R, Claudon M, Roy C, Mège-Lechevallier F, *et al*. Use of prostate systematic and targeted biopsy on the basis of multiparametric MRI in biopsy-naive patients (MRI-FIRST): a prospective, multicentre, paired diagnostic study. The Lancet Oncology. 2019; 20: 100–109.

[13] Weinreb JC, Barentsz JO, Choyke PL, Cornud F, Haider MA, Macura KJ, *et al*. PI-RADS prostate imaging—reporting and data system: 2015, version 2. European Urology. 2016; 69: 16–40.

[14] Li M, Yang L, Yue Y, Xu J, Huang C, Song B. Use of radiomics to improve diagnostic performance of PI-RADS v2.1 in prostate cancer. Frontiers in Oncology. 2020; 10: 631831.

[15] Duenweg SR, Bobholz SA, Barrett MJ, Lowman AK, Winiarz A, Nath B, *et al*. T2-weighted MRI radiomic features predict prostate cancer presence and eventual biochemical recurrence. Cancers. 2023; 15: 4437.

[16] Franco PN, Frade-Santos S, García-Baizán A, Paredes-Velázquez L, Aymerich M, Sironi S, *et al*. An MRI assessment of prostate cancer local recurrence using the PI-RR system: diagnostic accuracy, inter-observer reliability among readers with variable experience, and correlation with PSA values. European Radiology. 2024; 34: 1790–1803.

[17] Nicoletti G, Mazzetti S, Maimone G, Cignini V, Cuocolo R, Faletti R, *et al*. Development and validation of an explainable radiomics model to predict high-aggressive prostate cancer: a multicenter radiomics study based on biparametric MRI. Cancers. 2024; 16: 203.

[18] Guo Z, Qin X, Mu R, Lv J, Meng Z, Zheng W, *et al*. Amide proton transfer could provide more accurate lesion characterization in the transition zone of the prostate. Journal of Magnetic Resonance Imaging. 2022; 56: 1311–1319.

[19] Tamada T, Kido A, Ueda Y, Takeuchi M, Fukunaga T, Sone T, *et al*. Clinical impact of ultra-high *b*-value (3000 s/mm^2) diffusion-weighted

magnetic resonance imaging in prostate cancer at 3T: comparison with *b*-value of 2000 s/mm^2. The British Journal of Radiology. 2022; 95: 20210465.

[20] Brembilla G, Giganti F, Sidhu H, Imbriaco M, Mallett S, Stabile A, *et al*. Diagnostic accuracy of abbreviated bi-parametric MRI (a-bpMRI) for prostate cancer detection and screening: a multi-reader study. Diagnostics. 2022; 12: 231.

[21] Tsuruta C, Hirata K, Kudo K, Masumori N, Hatakenaka M. DWI-related texture analysis for prostate cancer: differences in correlation with histological aggressiveness and data repeatability between peripheral and transition zones. European Radiology Experimental. 2022; 6: 1.

[22] Messina E, Pecoraro M, Laschena L, Bicchetti M, Proietti F, Ciardi A, *et al*. Low cancer yield in PI-RADS 3 upgraded to 4 by dynamic contrast-enhanced MRI: is it time to reconsider scoring categorization? European Radiology. 2023; 33: 5828–5839.

[23] Tavakoli AA, Hielscher T, Badura P, Görtz M, Kuder TA, Gnirs R, *et al*. Contribution of dynamic contrast-enhanced and diffusion MRI to PI-RADS for detecting clinically significant prostate cancer. Radiology. 2023; 306: 186–199.

[24] Iyama Y, Nakaura T, Katahira K, Iyama A, Nagayama Y, Oda S, *et al*. Development and validation of a logistic regression model to distinguish transition zone cancers from benign prostatic hyperplasia on multi-parametric prostate MRI. European Radiology. 2017; 27: 3600–3608.

[25] Dinis Fernandes C, van Houdt PJ, Heijmink SWTPJ, Walraven I, Keesman R, Smolic M, *et al*. Quantitative 3T multiparametric MRI of benign and malignant prostatic tissue in patients with and without local recurrent prostate cancer after external-beam radiation therapy. Journal of Magnetic Resonance Imaging. 2019; 50: 269–278.

[26] Sun H, Du F, Liu Y, Li Q, Liu X, Wang T. DCE-MRI and DWI can differentiate benign from malignant prostate tumors when serum PSA is ≥10 ng/mL. Frontiers in Oncology. 2022; 12: 925186.

[27] Winkel DJ, Heye TJ, Benz MR, Glessgen CG, Wetterauer C, Bubendorf L, *et al*. Compressed sensing radial sampling MRI of prostate perfusion: utility for detection of prostate cancer. Radiology. 2019; 290: 702–708.

[28] Børretzen A, Reisæter LAR, Ringheim A, Gravdal K, Haukaas SA, Fasmer KE, *et al.* Microvascular proliferation is associated with high tumour blood flow by mpMRI and disease progression in primary prostate cancer. Scientific Reports. 2023; 13: 17949.

[29] Uysal A, Karaosmanoğlu AD, Karcaaltıncaba M, Akata D, Akdogan B, Baydar DE, *et al*. Prostatitis, the great mimicker of prostate cancer: can we differentiate them quantitatively with multiparametric MRI? American Journal of Roentgenology. 2020; 215: 1104–1112.

[30] Chen T, Zhang Z, Tan S, Zhang Y, Wei C, Wang S, *et al.* MRI based radiomics compared with the PI-RADS V2.1 in the prediction of clinically significant prostate cancer: biparametric vs multiparametric MRI. Frontiers in Oncology. 2021; 11: 792456.

[31] Rapisarda S, Bada M, Crocetto F, Barone B, Arcaniolo D, Polara A, *et al*. The role of multiparametric resonance and biopsy in prostate cancer detection: comparison with definitive histological report after laparoscopic/robotic radical prostatectomy. Abdominal Radiology. 2020; 45: 4178–4184.

[32] Gentile F, La Civita E, Della Ventura B, Ferro M, Cennamo M, Bruzzese D, *et al*. A combinatorial neural network analysis reveals a synergistic behaviour of multiparametric magnetic resonance and prostate health index in the identification of clinically significant prostate cancer. Clinical Genitourinary Cancer. 2022; 20: e406–e410.

How to cite this article: Chengcheng Gao, Yangsheng Li, Chunfeng Hu, Gang Tao, Jingyi Huang. The significance of PI-RADS v2.1 score combined with quantitative parameters of DWI and DCE-MRI in differentiating between benign prostatic hyperplasia and prostate cancer. Journal of Men's Health. 2024; 20(9): 95-102. doi: 10.22514/jomh.2024.154.